

The evolution of strictly monofunctional naphthoquinol *C*-methyltransferases is vital in cyanobacteria and plastids

Lauren Stutts , Scott Latimer, Zhaniya Batyrshina, Gabriella Dickinson, Hans Alborn, Anna K. Block and Gilles J. Basset

- 1 Department of Horticultural Sciences, University of Florida, Gainesville, FL 32611, USA
- 2 Center for Medical, Agricultural and Veterinary Entomology, ARS, USDA, Gainesville, FL 32608, USA

*Author for correspondence: gbasset@ufl.edu

The author responsible for distribution of materials integral to the findings presented in this article in accordance with the policy described in the Instructions for Authors (https://academic.oup.com/plcell/pages/General-Instructions) is: Gilles J. Basset (gbasset@ufl.edu).

Abstract

Prenylated quinones are membrane-associated metabolites that serve as vital electron carriers for respiration and photosynthesis. The UbiE (EC 2.1.1.201)/MenG (EC 2.1.1.163) C-methyltransferases catalyze pivotal ring methylations in the biosynthetic pathways of many of these quinones. In a puzzling evolutionary pattern, prokaryotic and eukaryotic UbiE/MenG homologs segregate into 2 clades. Clade 1 members occur universally in prokaryotes and eukaryotes, excluding cyanobacteria, and include mitochondrial COQ5 enzymes required for ubiquinone biosynthesis; Clade 2 members are specific to cyanobacteria and plastids. Functional complementation of an Escherichia coli ubiE/menG mutant indicated that Clade 1 members display activity with both demethylbenzo-quinols and demethylnaphthoquinols, independently of the quinone profile of their original taxa, while Clade 2 members have evolved strict substrate specificity for demethylnaphthoquinols. Expression of the gene-encoding bifunctional Arabidopsis (Arabidopsis thaliana) COQ5 in the cyanobacterium Synechocystis or its retargeting to Arabidopsis plastids resulted in synthesis of a methylated variant of plastoquinone-9 that does not occur in nature. Accumulation of methylplastoquinone-9 was acutely cytotoxic, leading to the emergence of suppressor mutations in Synechocystis and seedling lethality in Arabidopsis. These data demonstrate that in cyanobacteria and plastids, co-occurrence of phylloquinone and plastoquinone-9 has driven the evolution of monofunctional demethylnaphthoquinol methyltransferases and explains why plants cannot capture the intrinsic bifunctionality of UbiE/MenG to simultaneously synthesize their respiratory and photosynthetic quinones.

Introduction

Catalytic promiscuity, together with gene duplications and mutations, is thought to be one of the key molecular mechanisms that underlies the emergence of novel metabolic capabilities (Jensen 1976; Carbonell et al. 2011). In this model, substrate-ambiguous enzymes generate an array of products, some of which confer a selective advantage; gene duplication and divergence then contribute to fixing the increase in fitness and to driving metabolic specialization (Jensen 1976; Carbonell et al. 2011). Moreover, evolution can capture catalytic

promiscuity to create metabolic switches, allowing cells to quickly respond to environmental changes (Jeffery 2004). A typical example of such a pivotal enzyme is the bifunctional UbiE (EC 2.1.1.201)/MenG (EC 2.1.1.163) *C*-methyltransferase that catalyzes ring methylations in the biosynthetic pathways of the electron carriers ubiquinone (coenzyme Q, a benzoquinone) and menaquinone (vitamin K2, a naphthoquinone) in some prokaryotes (Lee et al. 1997; Fig. 1). This enzyme operates at a critical metabolic node, because bacteria must coordinate the respective proportions of ubiquinone, menaquinone, and its unmethylated precursor, demethylmenaquinone, depending on oxygen

IN A NUTSHELL

Background: Prenylated quinones are membrane-associated metabolites that carry electrons in respiration and photosynthesis. Some of them double as antioxidants and vitamins. Most quinones fall within 2 chemical families: the benzoquinones (e.g. ubiquinone and plastoquinone-9) and the naphthoquinones (e.g. phylloquinone and menaquinone). Furthermore, some prenylated quinones (such as ubiquinone and phylloquinone) carry a methyl group on their quinone ring at the position adjacent to the prenyl side chain, while others (such as plastoquinone-9 and demethylmenaquinone) lack this substitution. The presence or absence of this methyl group is functionally critical and is determined by the activity of an enzyme called quinone *C*-methyltransferase. Some prokaryotes use the same quinone *C*-methyltransferase to synthesize benzoquinones and naphthoquinones.

Question: Do plants, like certain bacteria, exploit the catalytic promiscuity of quinone *C*-methyltransferases to synthesize both ubiquinone and phylloquinone?

Findings: Phylogenetic reconstructions showed that quinone *C*-methyltransferases segregate into 2 clades. Clade 1 members are distributed throughout eukaryotic and prokaryotic lineages, excluding cyanobacteria, and include mitochondrial *C*-methyltransferases required for ubiquinone biosynthesis. Clade 2 members, in contrast, are specific to cyanobacteria and plastids, where they are required for the biosynthesis of phylloquinone. Functional complementation assays in *Escherichia coli* indicated that Clade 1 enzymes can methylate both benzoquinones and naphthoquinones, but Clade 2 members only methylate naphthoquinones. Expressing a bifunctional Clade 1 enzyme in the cyanobacterium *Synechocystis* or in *Arabidopsis* (*Arabidopsis thaliana*) plastids produced a new-to-nature methylated variant of plastoquinone-9. Methylplastoquinone-9 behaved as an antimetabolite of plastoquinone-9 and inhibited photosynthesis. These data demonstrate that in cyanobacteria and plastids, the presence of plastoquinone-9 acts as a selective force for the emergence of strictly monofunctional demethylnaphthoquinol methyltransferases.

Next steps: The discovery that methylplastoquinone-9 is a potent antimetabolite of plastoquinone-9 offers prospects for discovering novel herbicides and algicides.

availability and carbon source (Unden 1988; Søballe and Poole 1999; Bekker et al. 2007).

Yeast and animals possess a homolog of prokaryotic UbiE/ MenG called COQ5 (Barkovich et al. 1997; Nguyen et al. 2014). The enzyme is targeted to mitochondria, where it contributes exclusively to the biosynthesis of ubiquinone (Fig. 1). In contrast, the genome of Arabidopsis (Arabidopsis thaliana) encodes 2 homologs of *UbiE/MenG*. The first one is a *COQ5* ortholog (At5g57300), and complementation assays have shown that expression of this gene restored ubiquinone biosynthesis in a yeast *coq5* knockout (Hayashi et al. 2014). High-throughput proteomic studies have also consistently identified Arabidopsis COQ5 in highly purified mitochondria preparations (Heazlewood et al. 2004; Senkler et al. 2017; Niehaus et al. 2020). The second homologous gene (At1g23360) encodes an enzyme that is targeted to plastids, where it catalyzes the methylation of demethylphylloquinol into phylloquinol (vitamin K1; Fig. 1), a structural analog of menaquinone that serves as the A1 electron acceptor of Photosystem I (Brettel et al. 1986; Lohmann et al. 2006; Fatihi et al. 2015). This enzyme, demethylphylloquinol methyltransferase (DPhQ-MT), is frequently referred to in the literature and in genomic databases as "MenG" by reference to the authentic Escherichia coli UbiE/MenG enzyme, although sensu stricto plants do not synthesize menaguinone (Lohmann et al. 2006; Fatihi et al. 2015). Furthermore, in some plants, specifically nonphotosynthetic parasitic species, DPhQ-MT orthologs

lack a chloroplast transit peptide and are targeted instead to the plasma membrane (Gu et al. 2021).

We initiated this study to explore whether plants, like bacteria, exploit the catalytic versatility of quinone C-methyltransferases to coordinate the operation of their electron transfer chains. For instance, since protein dual targeting to mitochondria and plastids is frequent in angiosperms, including for phylloquinone biosynthesis (Eugeni Piller et al. 2011; Xu et al. 2013), some taxa could have evolved a single bifunctional COO5/DPhO-MT that participates in both ubiquinone and phylloquinone biosynthesis. Alternatively, quinone C-methyltransferase orthologs might be targeted to mitochondria in some taxa and to plastids in others. Plant COO5 or DPhO-MT could also have evolved from different bacterial progenitors, via independent events of horizontal gene transfer, depending on the plant lineages. There are precedents for this scenario in the assembly and prenylation of the naphthoquinone moiety of phylloquinone in photosynthetic eukaryotes (Gross et al. 2008; Widhalm et al. 2012).

Here, we present phylogenetic and biochemical evidence indicating that the evolutionary history of plant quinone *C*-methyltransferases strictly corresponds to their respective target organelles and function. We then combine reverse genetics and synthetic biology approaches in cyanobacteria and *Arabidopsis* to demonstrate that oxygenic photosynthetic organisms have evolved monofunctional DPhQ-MT

Figure 1. Benzoquinone and naphthoquinone ring methylations in the biosynthetic pathways of ubiquinone, menaquinone, and phylloquinone. A) Prokaryotic UbiE/MenG and mitochondrial COQ5 catalyze the C-methylation of the intermediate 2-methoxy-6-all-trans-polyprenyl-1,4-benzoquinol (1) into 6-methoxy-3-methyl-2-all-trans-polyprenyl-1,4-benzoquinol (2) in the biosynthetic pathway of ubiquinone. B) Prokaryotic UbiE/MenG and DPhQ-MT catalyze the last step in the biosynthetic pathways of menaquinone and phylloquinone, respectively. R", all trans-prenyl moieties of variable length (e.g. R' = octaprenyl in E. coli; R' = solanesyl in E. coli; R'' = octaprenyl in plants). AdoMet, S-adenosyl-L-methionine; AdoHcy, S-adenosyl-L-homocysteine.

and explain the molecular basis of the selective force that drives this strict substrate specificity.

Results

Quinone *C*-methyltransferases of plastids and mitochondria display strict phylogenetic segregation

A survey of fully sequenced genomes sampled throughout angiosperms, lycophytes, bryophytes, and chlorophytes showed that the corresponding taxa all harbored at least 2 close homologs of prokaryotic UbiE/MenG and that these proteins clustered in 2 phylogenetic clades (Fig. 2; Supplemental Table S1). The first clade includes orthologs of *Arabidopsis*, human, and yeast (*Saccharomyces cerevisiae*) COQ5 proteins and some UbiE/MenG proteins from eubacteria, excluding cyanobacteria (Fig. 2). The second clade exclusively comprises plant and cyanobacterial proteins and includes experimentally confirmed DPhQ-MT from *Arabidopsis* and *Synechocystis* sp. PCC 6803 (Fig. 2). Emergence of paralogs is frequent in both clades (Fig. 2).

Overlaying known and predicted subcellular localizations onto this phylogenetic reconstruction indicated that all the eukaryotic members from the first clade are targeted exclusively to the mitochondrion (Fig. 2; Supplemental Table S1). In contrast, the majority of plant proteins from the second clade are either known (*Arabidopsis*) or predicted to be targeted to plastids (Fig. 2; Supplemental Table S1). The few exceptions are 3 proteins from green algae (*Bathycoccus prasinos, Micromonas commoda*, and *Ostreococcus tauri*) and 4 paralogs in angiosperms (1 each in tobacco [*Nicotiana tabacum*] and soybean [*Glycine max*] and 2 in wheat [*Triticum*

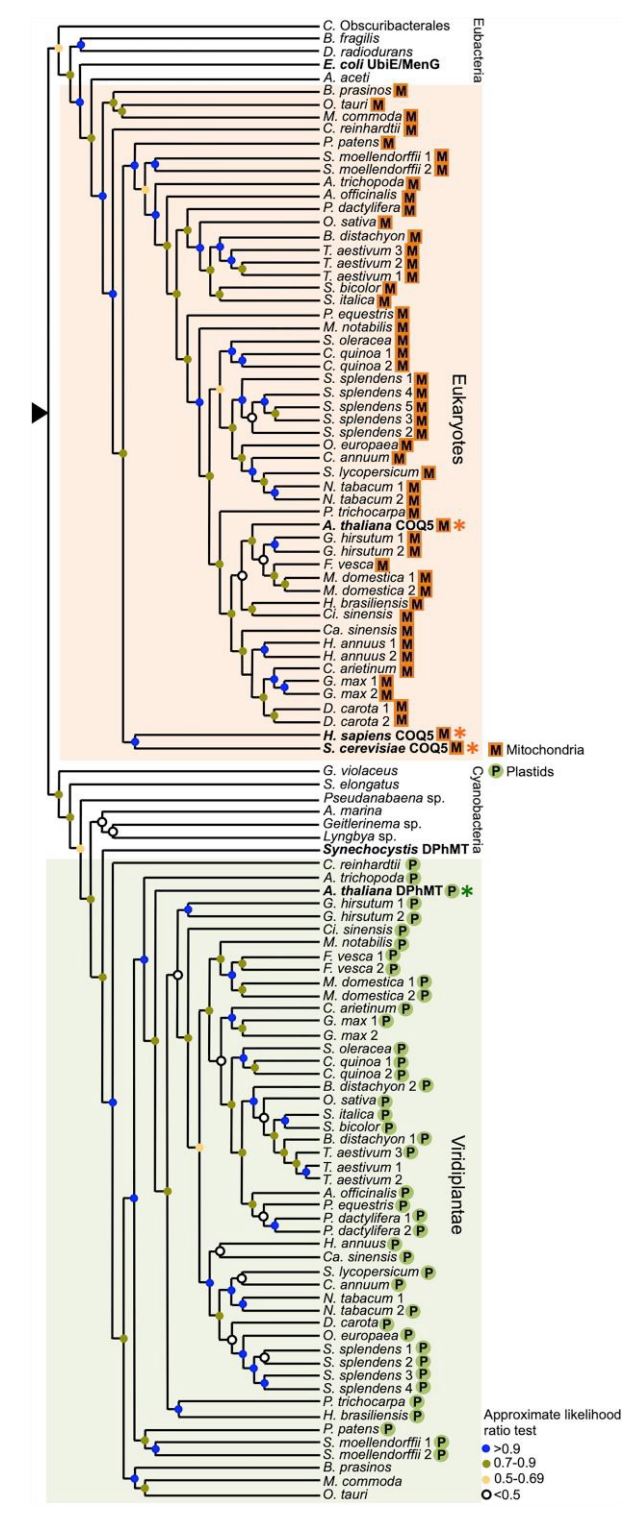


Figure 2. Maximum-likelihood reconstruction of the phylogenetic relationships of quinone *C*-methyltransferases mined from prokaryotic and eukaryotic genomes using *E. coli* UbiE/MenG as a query. The triangle marks the position of the outgroup. Colored dots indicate value ranges from an approximate likelihood-ratio test for branch support. Asterisks indicate that subcellular localization to the target organelle has been experimentally verified. Accession numbers and individual results from subcellular prediction algorithms are given in Supplemental Table S1.

aestivum]), for which no consensus subcellular targeting was found (Fig. 2; Supplemental Table S1). For all angiosperms, at least 1 paralog is predicted to be targeted to plastids (Fig. 2; Supplemental Table S1). In the case of the 3 algal proteins, failure to robustly infer subcellular localization is likely attributable to algorithm bias: there is indeed evidence that sequence-based prediction tools, which have been predominantly trained with land plant proteins, fail to detect many plastid targeted proteins in chlorophytes (Tardif et al. 2012).

It therefore appears that, unlike bacteria, plants have evolved separate *C*-methyltransferases to synthesize their benzoquinones and naphthoquinones. Not only is the evolutionary scenario of a single quinone *C*-methyltransferase that is dual targeted to mitochondria and plastids never observed, but also no clade 1 enzyme appears to be targeted to plastids and conversely no Clade 2 enzyme appears to be targeted to mitochondria.

Clade 2 *C*-methyltransferases have evolved strict substrate specificity for prenylated naphthoguinols

Having shown that a hidden selection pressure operated throughout plant lineages to keep quinone C-methyltransferases of plastids evolutionarily and spatially separate from those of mitochondria, we screened a sample of Clade 1 and Clade 2 enzymes via functional complementation of an E. coli \(\Delta ubiE/menG \) knockout strain. This E. coli mutant is unable to catalyze the methylation of the biosynthetic intermediates of prenylated naphthoguinones and prenylated benzoquinones (Fig. 1) and therefore is devoid of menaquinone-8 and ubiquinone-8 (Table 1). Complementation with Clade 1 enzymes from prokaryotes and truncated eukaryotic orthologs-i.e. without mitochondrial presequence—resulted in the production of menaquinone-8 and ubiquinone-8, while complementation with Clade 2 enzymes from cyanobacteria and truncated plant orthologs—i.e. without plastid transit peptide—produced menaquinone-8 only (Table 1). No quinone formation was detected with the Clade 1 orthologs of Physcomitrium patens and M. commoda or with the Clade 2 orthologs of P. patens, O. tauri, and M. commoda indicating that these enzymes were not functional in E. coli (Table 1). These results demonstrate that cyanobacterial quinone C-methyltransferases and their plastid-targeted orthologs act on prenylated naphthoquinols, but not on prenylated benzoquinols.

Also remarkable is the observation that the bifunctionality of Clade 1 enzymes is independent of the type of prenylated quinones produced by the organism of origin. For instance, *Bacillus fragilis* and *Deinococcus radiodurans* are exclusive menaquinone producers, while *Acetobacter aceti* produces exclusively ubiquinone (Collins and Jones 1981). Similarly, yeast and humans synthesize ubiquinone, but not menaquinone or phylloquinone.

COQ5 expression in cyanobacteria and COQ5 retargeting to plastids results in acute cytotoxicity

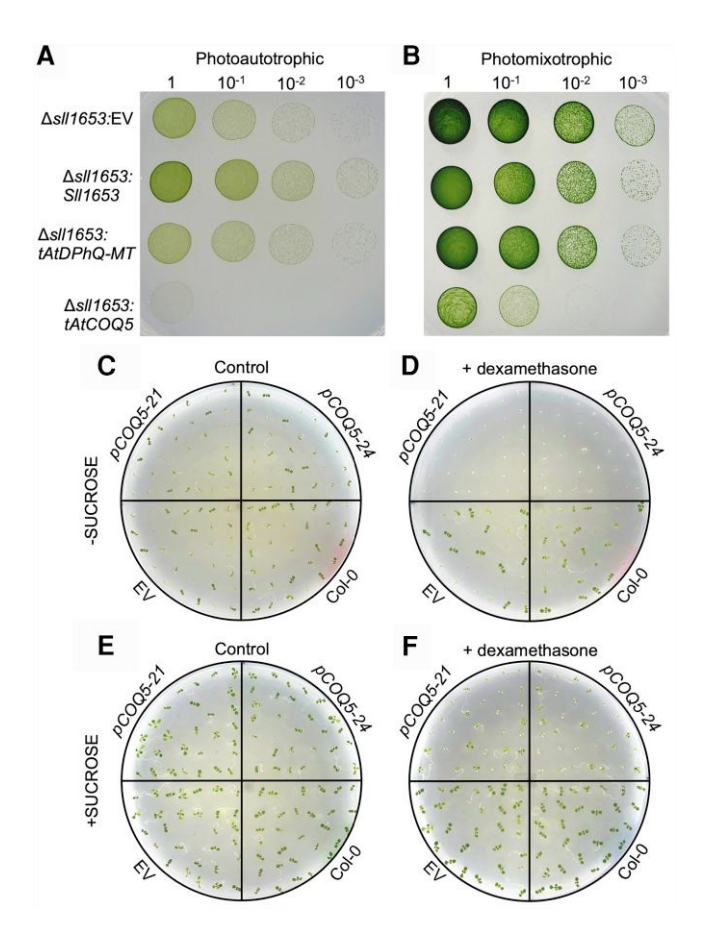
To further investigate why Clade 2 C-methyltransferases evolved strict substrate preferences, we examined the effect

Table 1. Complementation of *E. coli* $\Delta ubiE$

	pmoles/unit OD ₆₀₀	
	Menaquinone-8	Ubiquinone-8
E. coli K12	11.7 ± 2.2	234.2 ± 20.9
E. coli ΔubiE/MenG	$n.\overline{d}$.	$n.\overline{d}$.
Clade 1		
S. cerevisiae (E44 \rightarrow M44)	96.3 ± 2.5	57.4 ± 2.8
H. sapiens (E46 \rightarrow M46)	320.8 ± 29.9	99.1 ± 8
A. thaliana (S23 \rightarrow M23)	102.4 ± 4.7	61.7 ± 9.6
Solanum lycopersicum (S25 → M25)	101.1 ± 5.2	39.1 ± 1.6
Spinacia oleracea (R23 → M23)	150.1 ± 5	46.8 ± 1.9
<i>Oryza sativa</i> (F29 → M29)	130.7 ± 5.7	97.2 ± 4.7
Amborella trichopoda (F23 → M23)	147.6 ± 5.4	91.2 ± 6
Selaginella moellendorffii (S24 →	122.9 ± 1.6	74 ± 1.2
M24)		
P. patens (S36 \rightarrow M36)	n.d.	n.d.
<i>O. tauri</i> (S66 → M66)	128.1 ± 4.5	67.2 ± 0.8
$M. commoda (A33 \rightarrow M33)$	n.d.	n.d.
E. coli	91.5 ± 3.2	195.6 ± 9.7
B. fragilis	157.8 ± 17.4	55.9 ± 5.1
A. aceti	262 ± 9.2	48.7 ± 3.2
D. radiodurans	142 ± 10.5	53.5 ± 4.9
C. Obscuribacteriales	108.3 ± 6.6	16.2 ± 0.4
Clade 2		
A. thaliana (V28 \rightarrow M28)	25.2 ± 1.9	n.d.
S. lycopersicum (L23 \rightarrow M23)	29.9 ± 1.2	n.d.
S. oleracea (I29 \rightarrow M29)	44.4 ± 0.4	n.d.
O. sativa (A29 \rightarrow M29)	3.5 ± 0.8	n.d.
A. trichopoda (S25 \rightarrow M25)	21.4 ± 4	n.d.
S. moellendorffii (A33 → M33)	52.3 ± 6.4	n.d.
P. patens (G75 \rightarrow M75)	n.d.	n.d.
$O. tauri (S60 \rightarrow M60)$	n.d.	n.d.
$M. commoda (S98 \rightarrow M98)$	n.d.	n.d.
S. sp. PCC6803	12.5 ± 2.1	n.d.
Synechococcus elongatus	31.4 ± 0.9	n.d.

The positions of truncations of mitochondrial presequences and plastid transit peptides are indicated in parentheses. Accession numbers are provided in Supplemental Table S1. Data are means of 3 biological replicates \pm SE. n.d., not detected.

of replacing cognate cyanobacterial and plastid-targeted DPhQ-MT with a bifunctional COQ5 counterpart. To do that, an N-terminally truncated version of Arabidopsis COO5 (tAtCOQ5) was first subcloned into cyanobacterial expression vector pSynExp-2 under the control of constitutive promoter psbA2. Native Synechocystis DPhQ-MT (Sll1653) and its N-terminally truncated *Arabidopsis* ortholog (tAtDPhQ-MT) served as positive controls and empty pSynExp-2 as the negative control. These constructs were then introduced into a Synechocystis DPhO-MT knockout strain, and the growth of individual clones was scored via serial dilution assays (Fig. 3, A and B). In photoautotrophic conditions, barely any growth was observed for the COO5-harboring cells even after 3 wk of incubation (Fig. 3A). After 8 to 10 wk of incubation, fast-growing colonies appeared in the corresponding inocula; sequencing of the COO5 insert in 3 of these colonies revealed the presence of either deletions in a COQ5/UbiE signature domain (IPRO23576) or of a single base insertion resulting in an early stop codon (Supplemental Fig. S1). When cells were cultured photomixotrophically, growth of the COQ5 transformant was



Quinone biosynthesis in phototrophs

Figure 3. Expression of *Arabidopsis COQ5* in *Synechocystis* and *Arabidopsis DPhQ-MT* knockout mutants. **A)**, **B)** Growth of *Synechocystis DPhQ-MT* knockout cells (Δ*sll1653*) on BG-11 medium. EV, empty vector; *tAtDPhQ-MT* and *tAtCOQ5*, N-terminally truncated versions of *Arabidopsis DPhQ-MT* (At1g23360) and COQ5 (At5g57300), respectively. **C)** to **F)** Ten-day-old *Arabidopsis AtDPhQ-MT* knockout plants grown on MS medium with or without 1% (w/v) sucrose and with or without 10 μM dexamethasone. *pCOQ5-21* and *pCOQ5-24* correspond to independent transgenic lines harboring plastid-targeted *Arabidopsis* COQ5 under the control of a dexamethasone-inducible promoter. EV, empty vector; Col-0, wild type.

readily observed but still displayed major delay as compared to that of control strains (Fig. 3B).

In parallel, an *Arabidopsis COQ5* cDNA, the mitochondrial presequence of which had been swapped for a plastid transit peptide (*pCOQ5*), was placed under the control of a dexamethasone-inducible promoter, and this construct was introduced into an *Arabidopsis DPhQ-MT* T-DNA knockout. When sowed on control plates, T3 seeds homozygous for the *COQ5* transgene (lines *pCOQ5-21* and *pCOQ5-24*) germinated and developed similarly to the empty vector and wild-type control seedlings (Fig. 3, C and E). In contrast, on dexamethasone-containing plates without sucrose, *COQ5* transgenics were fully chlorotic and stopped growing immediately after emergence of the cotyledons (Fig. 3D). These developmental defects were attenuated when sucrose was added to the culture medium (Fig. 3F). No difference in

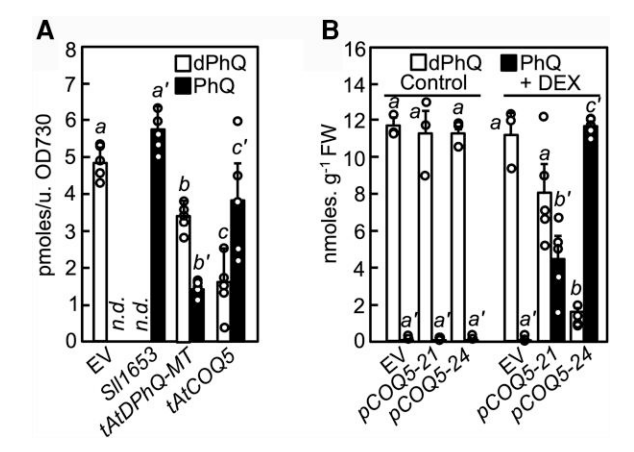


Figure 4. Analyses of prenylated naphthoquinones in *Synechocystis* and *Arabidopsis demethylphylloquinol methytransferase* knockout mutants. **A)** Demethylphylloquinone (dPhQ) and phylloquinone (PhQ) content in *Synechocystis* cells grown photomixotrophically. EV, empty vector; *Sll1653*, native *Synechocystis* DPhQ-MT; tAtDPhQ-MT and tAtCOQ5, N-terminally truncated versions of *Arabidopsis DPhQ-MT* (At1g23360) and COQ5 (At5g57300), respectively. **B)** Demethylphylloquinone (dPhQ) and phylloquinone (PhQ) content in *Arabidopsis* rosette leaves. EV, empty vector; pCOQ5-21 and pCOQ5-24, plastid-targeted *Arabidopsis* COQ5 (dexamethasone-inducible). Data are means of 3 to 5 biological replicates \pm SE. *n.d.*, not detected. Different letters indicate statistically significant differences as calculated by Tukey's test (P < 0.05). Prime annotations refer to phylloquinone. Statistics calculations are provided in Supplemental Table S2.

phenotype and growth was observed between control and dexamethasone-containing plates for the empty vector and wild-type controls (Fig. 3, C and D to F). These data demonstrate that replacing monofunctional DPhQ-MT with bifunctional COQ5 in cyanobacteria and plastids markedly impairs cell growth and viability. Furthermore, that the exogenous supply of carbohydrates mitigates such developmental defects suggests that *COQ5* expression is linked to impaired photosynthesis.

COQ5-harboring *Synechocystis* and *Arabidopsis* transgenics accumulate a methylated form of plastoquinone that does not exist in nature

Metabolite profiling targeted to vital photosynthetic quinones readily detected phylloquinone in the *Synechocystis* and soil-grown *Arabidopsis DPhQ-MT* knockouts that expressed *COQ5*, verifying that truncated COQ5 and plastid-targeted COQ5 versions were indeed catalytically active (Fig. 4, A and B). Conversion of demethylphylloquinone into phylloquinone represented ~70% of the total naphthoquinone pool in *Synechocystis* COQ5 transformants and ~37% (line *COQ5-21*) to ~88% (line *COQ5-24*) in their *Arabidopsis* counterparts (Fig. 4, A and B). As expected, phylloquinone was not detected in either of the vector alone controls or in the plants treated with the control spray (Fig. 4, A and B).

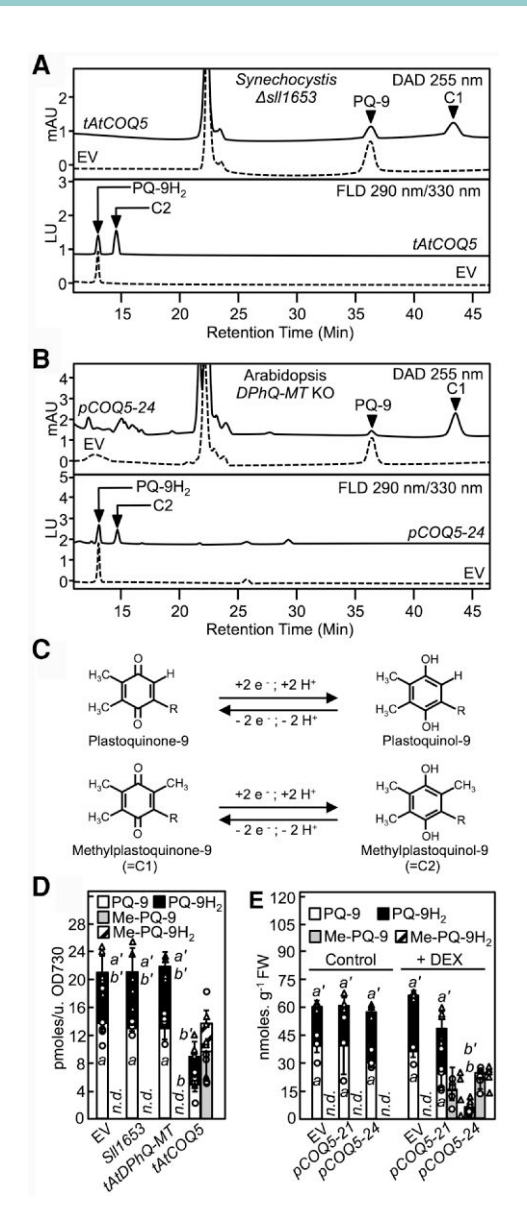


Figure 5. Analyses of plastoquinones in Synechocystis and Arabidopsis DPhO-MT knockout mutants. A) HPLC chromatograms with diode array (DAD 255 nm) and fluorimetric detections (FLD 290/330 nm) corresponding to extracts of Synechocystis DPhQ-MT knockout mutant strain (\Delta strain (\Delta strain (\Delta strain (\Delta strain (\Delta strain strain (\Delta strain str tCOQ5 expression construct (solid trace). C1, Compound 1; C2, Compound 2; plastoquinol-9 (PQ-9H₂); plastoquinone-9 (PQ-9). **B)** HPLC chromatograms with diode array and fluorimetric detections corresponding to extracts of Arabidopsis DPhQ-MT T-DNA knockout harboring either EV (dashed trace) or plastid-targeted Arabidopsis COQ5 expression construct (pCOQ5-24, solid trace). C) Structures of plastoquinone-9 and methylplastoquinone-9 (Compound 1) and their reduced versions, plastoquinol-9 and methylplastoquinol-9 (C2). R = solanesyl. **D),** E) Quantification of plastoquinone-9 (PQ-9), plastoquinol-9 (PQ-9H₂), methylplastoquinone-9 (Me-PQ-9), and methylplastoquinol-9 (Me-PQ-9H₂) in Synechocystis cells and Arabidopsis rosette leaves. Data are means of 3 to 5 biological replicates \pm ©. n.d., not detected. Different letters indicate statistically significant differences as calculated by Tukey's test (P < 0.05). Prime annotations refer to PQ-9H₂. Statistics calculations are provided in Supplemental Table S3. EV, empty vector.

HPLC separation combined with diode array and fluorescence spectrophotometry detected 2 unknown compounds, absent from either of the vector alone controls, in the extracts of COO5-expressing Synechocystis cells and Arabidopsis leaves (dexamethasone-treated line COQ5-24) (Fig. 5, A and B). The first compound (44.3 min) was detected adjacent to plastoquinone-9 (37 min), while the second compound (14.6 min) was detected adjacent to plastoquinol-9 (13.1 min), the reduced form of plastoquinone-9 (Fig. 4, A and B). When HPLC-purified Compound 1 was treated with sodium borohydride and then rechromatographed, its retention time was shifted to that of Compound 2 and displayed the same fluorescent characteristics, demonstrating that Compounds 1 and 2 obeyed the same redox chemistry as plastoquinone-9 and plastoquinol-9 (Supplemental Fig. S2). Given the catalytic promiscuity of COQ5 and the structural similarity between plastoquinone-9 (Fig. 5C) and COQ5's native benzoquinone substrate (Fig. 1A), we inferred that Compounds 1 and 2 likely corresponded to the methylated variants of plastoquinone-9 and plastoquinol-9 (Fig. 5C). High-resolution liquid chromatography (LC)-MS and targeted LC-MS/MS analyses confirmed that the masses of the parent and ring-containing product ions corresponding to Compound 1 extracted from Synechocystis and Arabidopsis were indeed identical to those predicted for methylplastoquinone-9 (Supplemental Figs. S3 to S5). Methylplastoquinone-9 and methylplastoquinol-9 were detected exclusively in the Synechocystis COO5 transformants and dexamethasone-treated Arabidopsis COO5 transgenics (Fig. 5, D and E). The accumulation of these methylated variants paralleled that of phylloquinone (Fig. 4, A and B) and was inversely correlated with the levels of plastoquinone-9 and plastoquinol-9 representing ~54% of the total benzoquinone pool in Synechocystis and ~25% (line COO5-21) to ~80% (line COQ5-24) in Arabidopsis (Fig. 5, D and E).

In contrast to plastoquinone-9, the oxidation level of which never exceeded ~60% in *Arabidopsis* leaves, methylplastoquinone-9 occurred predominantly in its oxidized form (83% and 92% oxidation in lines *COQ5-21* and *COQ5-24*, respectively) suggesting that the contribution of this methyl variant to the reactions of oxidoreduction in vivo is marginal (Fig. 5, D and E).

Five days after dexamethasone induction, transgenics from line *COQ5-24*, which displayed the largest conversion of plastoquinone-9 into methylplastoquinone-9, developed a bleaching phenotype (Supplemental Fig. S6). Imaging of chlorophyll *a* fluorescence and calculation of associated photosynthetic parameters indicated a collapse of maximum quantum efficiency of Photosystem II in dexamethasonetreated *COQ5-24* plants resulting in 10% photoinhibition (Table 2). Net CO₂ assimilation, which correlates with variable fluorescence decrease ratio (Lichtenthaler and Miehé 1997), and the ability to mitigate excess excitation energy via nonphotochemical quenching (Müller et al. 2001) were also significantly decreased in the induced *COQ5-24* transgenics as compared to the noninduced control plants

Table 2. Fluorescence parameters of *Arabidopsis* transgenics

•	Empty vector	pCOQ5-24
	Empty vector	pc0Q3-24
110 μ E m ⁻² s ⁻¹		
-DEX		
Fv/Fm	0.83 ± 0	0.83 ± 0
$R_{ m fd}$	1.12 ± 0.04	1.13 ± 0.03
NPQ	0.46 ± 0.02	0.46 ± 0.02
+DEX		
Fv/Fm	0.83 ± 0	$0.75 \pm 0.01*$
$R_{ m fd}$	1.11 ± 0.03	$0.39 \pm 0.04*$
NPQ	0.46 ± 0.01	$0.1 \pm 0.01*$
Photoinhibition (%)	0	10 ± 1**
800 μ E m ⁻² s ⁻¹ (72 h)		
-DEX		
Fv/Fm	0.82 ± 0	0.82 ± 0
$R_{ m fd}$	0.27 ± 0.02	0.28 ± 0.01
NPQ	0.21 ± 0.01	0.23 ± 0.01
+DEX		
Fv/Fm	0.82 ± 0	$0.26 \pm 0.04*$
$R_{ m fd}$	0.26 ± 0.02	$0.14 \pm 0.02*$
NPQ	0.20 ± 0.01	$0.15 \pm 0.02*$
Photoinhibition (%)	0	$68 \pm 5**$
800 μ E m ⁻² s ⁻¹ (120 h)		
-DEX		
Fv/Fm	0.83 ± 0	0.83 ± 0
$R_{ m fd}$	0.38 ± 0.02	0.38 ± 0.02
NPQ	0.23 ± 0.01	0.23 ± 0.01
+DEX		
Fv/Fm	0.83 ± 0	-
$R_{ m fd}$	0.35 ± 0.02	-
NPQ	0.24 ± 0.01	-
CPhotoinhibition (%)	0	=

Maximum quantum efficiencies (Fv/Fm), variable fluorescence decrease ratios ($R_{\rm fd}$), nonphotochemical quenching (NPQ) values, and percentages of photoinhibition in dexamethasone-induced (+DEX) plants versus noninduced controls (-DEX) were calculated from 20 measurements from 4 biological replicates \pm st.. Single asterisks indicate significant differences from the corresponding noninduced plants as determined by Fisher's test (P < 0.05) from an analysis of variance (Supplemental Table S4). For photoinhibition, double asterisks indicate significant differences from the corresponding empty vector control as determined by Fisher's test (P < 0.05) from an analysis of variance.

(Table 2). High-light treatment, which triggers a boost in the production of photoprotective plastoquinol-9 (Szymańska and Kruk 2010), exacerbated the bleaching phenotype and photosynthetic defects in the induced *COQ5-24* transgenics (Table 2; Supplemental Fig. S6). Photoinhibition reached 68% after 72 h of high-light treatment, and 48 h later, the entire leaf rosette had fully senesced (Table 2; Supplemental Fig. S6).

Discussion

Monofunctional demethylnaphthoquinol *C*-methyltransferases appear to be unique to oxygenic photosynthetic organisms

Here, we uncover the existence of a selection pressure that drives the evolution of quinol *C*-methyltransferases with strict specificity for demethylnaphthoquinol substrates in cyanobacteria and plastids. In contrast, UbiE/COQ5 homologs, whose taxonomic distribution is near universal, are

active with both demethylnaphthoquinol and benzoquinol substrates, irrespective of the quinone profile of their host organisms. From an evolutionary perspective, these findings are congruent with the observation that promiscuous enzymes tend to be uniformly distributed throughout the Tree of Life, while highly specific enzymes usually cluster in discrete lineages (Carbonell et al. 2011). In terms of catalytic mechanism, plant and cyanobacterial naphthoquinol methyltransferases have no wobble for substrate preference and thus represent evolutionary termini in the quinone C-methyltransferase family. Phylogenetic reconstructions and functional complementation assays indicate that monofunctional naphthoquinol methyltransferases most likely emerged in cyanobacteria, and that plastid-targeted orthologs are without exception of cyanobacterial descent (Fig. 2; Table 1). The finding that C. Obscuribacteriales bacterium, a member of the phylum of nonphotosynthetic bacteria (Melainabacteria) most closely related to cyanobacteria (Di Rienzi et al. 2013), harbors a bifunctional Clade 1 quinone C-methyltransferase, and no monofunctional Clade 2 ortholog validates this scenario (Fig. 2; Table 1).

The co-occurrence of phylloquinone and plastoquinone-9 in cyanobacteria and plastids drove the emergence of monofunctional naphthoquinol methyltransferases

Our results also demonstrate that, in cyanobacteria and plastids, the evolution and retention of monofunctional demethylnaphthoguinol methyltransferases are driven by the spatial co-occurrence of 2 vital redox cofactors. The first one is a prenylated naphthoguinone (phylloguinone or menaquinone depending on the organism) that functions as the electron acceptor A_1 of Photosystem I. The presence of a methyl group on carbon 2 of the naphthalene ringi.e. ortho of the prenyl chain (Fig. 1)—has been shown to be required for optimal photosynthetic activity (Lohmann et al. 2006; Fatihi et al. 2015). The second redox cofactor, plastoquinone-9, is a prenylated benzoquinone that serves multiple roles associated with photosynthesis, including electron transfer between Photosystem II and cytochrome b6/f. proton translocation through thylakoidal membranes, chlororespiration, cyclic electron flow, phytoene desaturation, redox sensing and signaling, and scavenging of reactive oxygen species (Havaux 2020). Importantly, unlike phylloquinone, menaquinone, or ubiquinone, plastoquinone-9 lacks a methyl group on the carbon ortho of the prenyl chain (Fig. 5C). The presence of bifunctional COQ5 in cyanobacteria or its retargeting to plastids results in the methylation of plastoquinone-9 at this ring position. Accumulation of methylplastoquinone-9 is acutely toxic, especially when transformants are cultured photoautrophically: Synechocystis clones eventually evolve suppressor mutations in the COQ5 gene, and dexamethasone-induced Arabidopsis transgenics are seedling lethal. These findings explain why in eukaryotes, the phylogenetic signals of quinone C-methyltransferases

rigidly track the target organelles of these enzymes and why plants in particular cannot capture the intrinsic bifunctionality of UbiE/COQ5 to synthesize simultaneously naphthoquinones and benzoquinones, as some prokaryotes do.

Methylplastoquinone-9 is a potent antimetabolite of plastoquinone-9

In Arabidopsis leaf tissues, methylplastoquinone-9 occurs almost exclusively in its oxidized form, in sharp contrast with the high quinol/quinone ratio that typifies the pool of photoactive plastoquinone-9 (Szymańska and Kruk 2010; Block et al. 2013). This result strongly suggests that methylplastoquinone-9 is not functional as an electron carrier for photosynthesis, and measurements of chlorophyll a fluorescence emission show indeed that the presence of plastidtargeted COQ5 triggers a pronounced drop of the maximum quantum efficiency of Photosystem II. There are indications. however, that the phenotypic defects associated with the accumulation of methylplastoquinone-9 go beyond the mere depletion of the photoactive pool of plastoquinone-9. Indeed, Arabidopsis solanesyl-diphosphate synthase mutants, for which loss of plastoquinone-9 is similar to that measured in the COQ5 transgenics, do not display any growth defects or impaired photosynthetic activity, at least when grown in a standard light regime (Block et al. 2013). It is therefore highly probable that, similar to the mode of action of an antimetabolite, methylplastoquinone-9 is itself cytotoxic, for instance by acting as a competitive inhibitor of plastoquinone-9 (e.g. Q_A binding site of Photosystem II, NADPH dehydrogenase complex, and plastid terminal oxidase). The situation is likely compounded in cyanobacteria, where plastoquinone-9 doubles as an electron carrier of the respiratory chain (Cooley and Vermaas 2001). From a biotechnology perspective, the discovery that methylplastoquinone-9 acts as a potent inhibitor of photosynthesis opens a new avenue for the development of novel herbicides and algicides.

Materials and methods

Bioinformatics

Prokaryotic and eukaryotic homologs of *E. coli* UbiE/MenG were mined from fully sequenced genomes using BLASTp searches. Phylogenetic reconstructions were performed using the following tool suite from NGPhylogeny.fr (Lemoine et al. 2019): MUSCLE (multiple alignment), Gblocks (removal of misaligned and divergent sequence regions), PhyML (tree inference via the maximum-likelihood method), and Newick Display (tree rendering). Sterol methyltransferases from *S. cerevisiae* (NP_013706.1) and *Arabidopsis* (*A. thaliana*, NP_0010785 79.1) served as an outgroup. Branch support was assessed via approximate likelihood-ratio test (Anisimova and Gascuel 2006). Subcellular localizations were predicted using TARGETP-2.0 (Almagro Armenteros et al. 2019), PREDOTAR (Small et al. 2004), WoLFPSORT (Horton et al. 2007), iPSORT (Bannai et al. 2002), and PredSL (Petsalaki et al. 2006).

Chemical and reagents

Standards of menaquinone-8, demethylmenaquinone-8, and ubiquinone-8 were prepared from *E. coli* K-12 extracts and HPLC purified (Kim et al. 2008; Latimer et al. 2021). Plastoquinone-9 and plastochromanol-8 were HPLC purified from *Arabidopsis* leaf extracts (Block et al. 2013). Demethylphylloquinone was extracted from the leaves of *Arabidopsis DPhQ-MT* knockout plants (GABI_565F06; Lohmann et al. 2006) and HPLC purified using the same method than that described for phylloquinone analysis in Widhalm et al. (2012). Ubiquinone-9 and ubiquinone-10 were from Sigma-Aldrich. Phylloquinone was from MP Biomedicals. Quinol standards were prepared by reduction of their corresponding quinone forms with 20 mm NaBH₄. Unless mentioned otherwise, other reagents were from Fisher Scientific.

Functional complementation of *E. coli*

The list of primers used for complementation of E. coli is provided as part of Supplemental Table S5. N-terminally truncated versions of cDNAs corresponding to Arabidopsis gene COO5 (At5g57300) and DPhQ-MT (At1g23360) were prepared from Arabidopsis Col-0 total leaf RNA using reverse transcription PCR (RT-PCR). N-terminally truncated S. cerevisiae COQ5 (E44 \rightarrow M44; YML110C) was PCR amplified from the genomic DNA of strain BY4741. E. coli gene ubiE/menG and Synechocystis DPhQ-MT (sll1653) were PCR amplified from the genomic DNA of E. coli K12 and Synechocystis sp. PCC 6803, respectively. All other DNAs were synthesized with codon optimization (Genescript, USA). Accession numbers of corresponding proteins and truncation positions are provided in Supplemental Table S1 and Table 1, respectively. DNAs were cloned into *EcoRI/XbaI*-digested pBAD24 (Guzman et al. 1995) using In-Fusion HD technology (Takara Bio) and introduced in E. coli ΔubiE778::kan (Keio strain JW5581-1; Baba et al. 2006). Keio strain JW5581-1 was obtained from CGSC (https://cgsc.biology.yale.edu). Empty pBAD24 was used as a negative control. Transformed cells were selected on LB plates containing ampicillin (100 μ g/mL) and kanamycin (50 μ g/mL).

Synechocystis transformation and Arabidopsis transgenics

The list of primers used for the construction of *Synechocystis* transformants and *Arabidopsis* transgenics is provided as part of Supplemental Table S5. For expression in *Synechocystis*, gene sll1653 and N-terminally truncated versions of At5g57300 (S23 \rightarrow M23) and At1g23360 (V28 \rightarrow M28) cDNAs were PCR amplified using primers that contained the NdeI (5') and BglII (3') restriction sites. PCR fragments were cloned into NdeI/BglII-digested pSynExp-2 expression vector (Sattler et al. 2003), and the resulting constructs were introduced into *Synechocystis* $\Delta sll653$::aadA knockout cells (Lohmann et al. 2006). Transformed cells were selected on BG-11 plates containing chloramphenicol

 $(5 \mu g/mL)$ and spectinomycin $(15 \mu g/mL)$ at 22 °C in 12-h days ($70 \,\mu\text{E m}^{-2} \text{ s}^{-1}$). For growth assays, 3-wk-old colonies were individually resuspended in 100 μL of BG11 medium, and serial dilutions were plated on BG-11 plates with or without 5 mm glucose. Plates were incubated in 12-h days (70 µE m⁻² s⁻¹) at 22 °C for 14 d (photomixotrophic conditions) or 21 d (photoautotrophic conditions). For targeting of Arabidopsis COQ5 into plastids, a cDNA sequence corresponding to At5g57300, the predicted mitochondrial presequence (residues 1 to 23) of which had been replaced by the transit peptide (79 amino acids) of a small subunit of Arabidopsis Rubisco (At1g67090; RBCS1A) was synthesized and codon optimized by GenScript, USA. This synthetic cDNA was subcloned using Gateway Technology (Invitrogen) into binary expression vector pOpOn (Peer et al. 2009). This construct and empty pOpOn control were transferred to Agrobacterium tumefaciens and then introduced into the *DPhQ-MT* knockout line via the floral dip method. Transformants were selected on MS solid medium containing kanamycin (50 μ g/mL) and 1% (w/v) sucrose. For induction of expression, dexamethasone was solubilized in DMSO and was used at the concentration of 10 μ m for experiments conducted on plates or at 20 µm, together with Silwet L-77 adjuvant (0.02% v/v), for spray treatments on soilgrown plants. Dexamethasone was omitted for the control treatments. Culture conditions were 12-h days (110 μ E m⁻² s⁻¹) at 22 °C for plants grown on plates and 12-h days (110 μ E m⁻² s⁻¹) or continuous high light (800 μ E m⁻² s⁻¹) at 22 °C for plants grown on soil. Induction and analyses of chlorophyll fluorescence were performed on 1-mo-old, dark-adapted plants using a FluorCam 800 MF imaging system (Photon Systems Instruments).

Metabolite analyses

For quinone analyses in E. coli, cells (20-mL cultures) were grown at 37 °C in LB medium containing 0.2% (w/v) arabinose as an inducer. Cells were harvested when cultures reached OD_{600} ~1 and washed once with sterile water at 4 °C. Resuspended cell pellets (1 mL) were quantified by absorbance at 600 nm. Cell disruption and analysis of corresponding extracts via reverse-phase HPLC coupled to diode array detection were performed as described in (Latimer et al. 2021). Ubiquinone-8 (9.5 min) was monitored at 275 nm. Demethylmenaquinone-8 (12.4 min) and menaquinone-8 (14 min) were monitored at 248 nm. Quinols were fully converted into their quinone forms during extraction and were therefore not detected. For the analyses of prenylated quinones in Synechocystis, cells were scooped from plates, quantified and disrupted as described in Fatihi et al. (2015). Ethanol extracts of *Arabidopsis* leaf tissues (30 to 80 mg) were prepared as described in Block et al. (2013). Benzoquinones were analyzed by reverse-phase HPLC as described in Block et al. (2013). Plastoquinol-9 (13.1 min) and methylplastoquinol-9 (14.6 min) were monitored fluorimetrically (290-nm excitation/330 emission). Plastoquinone-9 (37 min) was monitored by absorbance at 255 nm.

Methylplastoquinone-9 (44.3 min) was initially monitored by absorbance at 255 nm and then quantified at 266 nm. Reverse-phase HPLC separation coupled to fluorimetric detection (238-nm excitation/426-nm emission) after in-line reduction of demethylphylloquinone (14.5 min) and phylloquinone (17.3 min) was performed as described in Widhalm et al. (2009). A Thermo TSQ Quantis mass spectrometer (Thermo Scientific) was utilized for initial tandem MS analyses, using electro spray, in positive ion mode, purged with nitrogen gas at 300 °C, capillary voltage of 4,000 V, and collision energy of 20 V. Two microliters of HPLC-purified quinone fractions were rechromatographed on a Zorbax Eclipse Plus C18 column (2.1 mm × 50 mm 1.8 micron; Agilent Technologies) held at 40 °C and developed isocratically with methanol containing 5 mm ammonium formate at a flow rate of 0.4 mL/min. Compounds of interest were monitored using single reaction monitoring of the $[M + NH4]^+$ ions; plastoquinone-9 (m/z 766.6/diagnostic MS2 ion m/z151) and methylplastoquinone-9 (m/z780.6/diagnostic MS2 m/ z165) eluted at 15.5 and 19.4 min, respectively. Parent and daughter ions of plastoquinone-9 and methylplastoquinone-9 were further analyzed on a Thermo Q Exactive mass spectrometer (Thermo Scientific) using the same chromatographic and ion source settings. Ammonium, sodium, and potassium adducts of the intact compounds were identified using full scan at m/z 730 to 800 for plastoquinone and m/z 750 to 850 for methylplastoquinone-9 combined with total ion MS2 fragment scan at 13.87 and 17.71 min respectively to establish the mass for characteristic daughter ions. The exact mass for the ammonium adducts ([M + NH4]⁺) and MS2 daughter ions were established using single ion monitoring (SIM) coupled with data-driven MS2 scans and a collision energy of 35 eV for plastoquinone-9 (m/z 766.654) and methylplastoquinone-9 (m/z 780.667).

Accession numbers

Sequence data from this article can be found in the GenBank/EMBL data libraries under the following accession numbers: *Arabidopsis* COQ5 (NP_200540.1), *DPhQ-MT* (NP_173750.3), and *Synechocystis* sp. PCC6903 *DPhQ-MT* (BAA16833.1).

Author contributions

L.S. and G.J.B. designed and performed the experiments, analyzed the data, and wrote the manuscript. S.L., Z.B., G.D., H.A, and A.K.B. designed and performed the experiments, analyzed the data, and contributed to the preparation of the manuscript.

Supplemental data

The following materials are available in the online version of this article.

Supplemental Figure S1. Sequence comparison of *Arabidopsis COQ5* (At5g57300) cDNAs recovered from

10-wk-old *Synechocystis* colonies grown in photoautotrophic conditions (Mutants 1, 2, and 3) with that of the original wild-type cDNA.

Supplemental Figure S2. Redox conversions of Compound 1 into Compound 2 and of plastoquinone-9 into plastoquinol-9.

Supplemental Figure S3. LC-MS analyses of the ions of plastoquinone-9 and methylplastoquinone-9.

Supplemental Figure S4. Chromatograms of the parent and daughter ions of plastoquinone-9 and methylplastoquinone-9.

Supplemental Figure S5. Tandem MS analysis of plastoquinone-9 and methylplastoquinone-9.

Supplemental Figure S6. Phenotype of *Arabidopsis* transgenics.

Supplemental Table S1. Accession numbers and predicted subcellular localizations of plant proteins used for phylogenetic reconstructions.

Supplemental Table S2. Statistics for Fig. 4.

Supplemental Table S3. Statistics for Fig. 5.

Supplemental Table S4. Statistics for Table 2.

Supplemental Table S5. PCR primers.

Supplemental File S1. Alignment file for Fig. 2.

Supplemental File S2. Tree file for Fig. 2.

Funding

This work was made possible in part by the National Science Foundation Grants MCB-1712608 and MCB-2216747 (to G.J.B.), and by the United States Department of Agriculture-Agriculture Research Services project 6036-11210-001-00D (to A.K.B).

Conflict of interest statement. None declared.

References

- Almagro Armenteros JJ, Salvatore M, Emanuelsson O, Winther O, von Heijne G, Elofsson A, and Nielsen H. Detecting sequence signals in targeting peptides using deep learning. Life Sci. Alliance. 2019:2(5): e201900429. https://doi.org/10.26508/lsa.201900429
- **Anisimova M, Gascuel O**. Approximate likelihood-ratio test for branches: a fast, accurate, and powerful alternative. Syst Biol. 2006:**55**(4):539–552. https://doi.org/10.1080/10635150600755453
- Baba T, Ara T, Hasegawa M, Takai Y, Okumura Y, Baba M, Datsenko KA, Tomita M, Wanner BL, Mori H. Construction of *Escherichia coli* K-12 in-frame, single-gene knockout mutants: the Keio collection. Mol Syst Biol. 2006:2(1):2006.0008. https://doi.org/10.1038/msb4100050
- Bannai H, Tamada Y, Maruyama O, Nakai K, Miyano S. Extensive feature detection of N-terminal protein sorting signals. Bioinformatics 2002:18(2):298–305. https://doi.org/10.1093/bioinformatics/18.2.298
- Barkovich RJ, Shtanko A, Shepherd JA, Lee PT, Myles DC, Tzagoloff A, Clarke CF. Characterization of the *COQ5* gene from *Saccharomyces cerevisiae*. Evidence for a C-methyltransferase in ubiquinone biosynthesis. J Biol Chem. 1997:272(14):9182–9188. https://doi.org/10.1074/jbc.272.14.9182
- Bekker M, Kramer G, Hartog AF, Wagner MJ, de Koster CG, Hellingwerf KJ, Teixeira de Mattos MJ. Changes in the redox state and composition of the quinone pool of *Escherichia coli* during

- aerobic batch-culture growth. Microbiology (Reading) 2007:**153**(6): 1974–1980. https://doi.org/10.1099/mic.0.2007/006098-0
- Block A, Fristedt R, Rogers S, Kumar J, Barnes B, Barnes J, Elowsky CG, Wamboldt Y, Mackenzie SA, Redding K, et al. Functional modeling identifies paralogous solanesyl-diphosphate synthases that assemble the side chain of plastoquinone-9 in plastids. J Biol Chem. 2013;288(38):27594–27606. https://doi.org/10.1074/jbc.M113.492769
- **Brettel K, Sétif P, Mathis P.** Flash-induced absorption changes in Photosystem I at low temperature: evidence that the electron acceptor A1 is vitamin K1. FEBS Lett. 1986:**203**(2):220–224. https://doi.org/10.1016/0014-5793(86)80746-3
- Carbonell P, Lecointre G, Faulon J-L. Origins of specificity and promiscuity in metabolic networks. J Biol Chem. 2011:286(51): 43994–44004. https://doi.org/10.1074/jbc.M111.274050
- Collins MD, Jones D. Distribution of isoprenoid quinone structural types in bacteria and their taxonomic implication. Microbiol Rev. 1981:45(2):316–354. https://doi.org/10.1128/mr.45.2.316-354.1981
- Cooley JW, Vermaas WF. Succinate dehydrogenase and other respiratory pathways in thylakoid membranes of *Synechocystis* sp. strain PCC 6803: capacity comparisons and physiological function. J Bacteriol. 2001:**183**(14):4251–4258. https://doi.org/10.1128/JB.183. 14.4251-4258.2001
- Di Rienzi SC, Sharon I, Wrighton KC, Koren O, Hug LA, Thomas BC, Goodrich JK, Bell JT, Spector TD, Banfield JF, et al. The human gut and groundwater harbor non-photosynthetic bacteria belonging to a new candidate phylum sibling to Cyanobacteria. eLife 2013:2:e01102. https://doi.org/10.7554/eLife.01102
- Eugeni Piller L, Besagni C, Ksas B, Rumeau D, Bréhélin C, Glauser G, Kessler F, and Havaux M. Chloroplast lipid droplet type II NAD(P) H quinone oxidoreductase is essential for prenylquinone metabolism and vitamin K1 accumulation. Proc Natl Acad Sci U S A. 2011:108(34):14354–14359. https://doi.org/10.1073/pnas.1104790108
- Fatihi A, Latimer S, Schmollinger S, Block A, Dussault PH, Vermaas WF, Merchant SS, Basset GJ. A dedicated type II NADPH dehydrogenase performs the penultimate step in the biosynthesis of vitamin K1 in *Synechocystis* and *Arabidopsis*. Plant Cell 2015:27(6): 1730–1741. https://doi.org/10.1105/tpc.15.00103
- Gross J, Meurer J, Bhattacharya D. Evidence of a chimeric genome in the cyanobacterial ancestor of plastids. BMC Evol. Biol. 2008:8(1):117. https://doi.org/10.1186/1471-2148-8-117
- Gu X, Chen IG, Harding SA, Nyamdari B, Ortega MA, Clermont K, Westwood JH, Tsai CJ. Plasma membrane phylloquinone biosynthesis in nonphotosynthetic parasitic plants. Plant Physiol. 2021;185(4):1443–1456. https://doi.org/10.1093/plphys/kiab031
- Guzman LM, Belin D, Carson MJ, Beckwith J. Tight regulation, modulation, and high-level expression by vectors containing the arabinose PBAD promoter. J Bacteriol. 1995:177(14):4121–4130. https://doi.org/10.1128/jb.177.14.4121-4130.1995
- Havaux M. Plastoquinone in and beyond photosynthesis. Trends Plant Sci. 2020:25(12):1252–1265. https://doi.org/10.1016/j.tplants.2020.06.011
- Hayashi K, Ogiyama Y, Yokomi K, Nakagawa T, Kaino T, Kawamukai M. Functional conservation of coenzyme Q biosynthetic genes among yeasts, plants, and humans. PLoS One 2014:9(6):e99038. https://doi.org/10.1371/journal.pone.0099038
- Heazlewood JL, Tonti-Filippini JS, Gout AM, Day DA, Whelan J, Millar AH. Experimental analysis of the Arabidopsis mitochondrial proteome highlights signaling and regulatory components, provides assessment of targeting prediction programs, and indicates plant-specific mitochondrial proteins. Plant Cell 2004:16(1):241–256. https://doi.org/10.1105/tpc.016055
- Horton P, Park KJ, Obayashi T, Fujita N, Harada H, Adams-Collier CJ, Nakai K. WoLF PSORT: protein localization predictor. Nucleic Acids Res. 2007:35(Web Server):W585–W587. https://doi.org/10.1093/nar/gkm259
- Jeffery CJ. Molecular mechanisms for multitasking: recent crystal structures of moonlighting proteins. Curr Opin Struct Biol. 2004:14(6): 663–668. https://doi.org/10.1016/j.sbi.2004.10.001

- Jensen RA. Enzyme recruitment in evolution of new function. Annu Rev Microbiol. 1976:30(1):409–425. https://doi.org/10.1146/ annurev.mi.30.100176.002205
- Kim HU, van Oostende C, Basset GJ, Browse J. The AAE14 gene encodes the *Arabidopsis* o-succinylbenzoyl-CoA ligase that is essential for phylloquinone synthesis and Photosystem-I function. Plant J. 2008:**54**(2):272–283. https://doi.org/10.1111/j.1365-313X.2008.03416.x
- Latimer S, Keene SA, Stutts LR, Berger A, Bernert AC, Soubeyrand E, Wright J, Clarke CF, Block AK, Colquhoun TA, et al. A dedicated flavin-dependent monooxygenase catalyzes the hydroxylation of demethoxyubiquinone into ubiquinone (coenzyme Q) in *Arabidopsis*. J Biol Chem. 2021:297(5):101283. https://doi.org/10.1016/j.jbc.2021. 101283
- Lee PT, Hsu AY, Ha HT, Clarke CF. A C-methyltransferase involved in both ubiquinone and menaquinone biosynthesis: isolation and identification of the *Escherichia coli* ubiE gene. J Bacteriol. 1997:**179**(5): 1748–1754. https://doi.org/10.1128/jb.179.5.1748-1754.1997
- Lemoine F, Correia D, Lefort V, Doppelt-Azeroual O, Mareuil F, Cohen-Boulakia S, Gascuel O. NGPhylogeny.fr: new generation phylogenetic services for non-specialists. Nucleic Acids Res. 2019:47(W1):W260-W265. https://doi.org/10.1093/nar/gkz303
- Lichtenthaler HK, Miehé JA. Fluorescence imaging as a diagnostic tool for plant stress. Trends Plant Sci. 1997:2(8):316–320. https://doi.org/ 10.1016/S1360-1385(97)89954-2
- Lohmann A, Schöttler MA, Bréhélin C, Kessler F, Bock R, Cahoon EB, Dörmann P. Deficiency in phylloquinone (vitamin K1) methylation affects prenyl quinone distribution, Photosystem I abundance, and anthocyanin accumulation in the *Arabidopsis* AtmenG mutant. J Biol Chem. 2006:281(52):40461–40472. https://doi.org/10.1074/jbc. M609412200
- Müller P, Li XP, Niyogi KK. Non-photochemical quenching. A response to excess light energy. Plant Physiol. 2001:125(4):1558–1566. https://doi.org/10.1104/pp.125.4.1558
- Nguyen TP, Casarin A, Desbats MA, Doimo M, Trevisson E, Santos-Ocaña C, Navas P, Clarke CF, Salviati L. Molecular characterization of the human COQ5 C-methyltransferase in coenzyme Q10 biosynthesis. Biochim Biophys Acta. 2014;1841(11):1628–1638. https://doi.org/10.1016/j.bbalip.2014.08.007
- Niehaus M, Straube H, Künzler P, Rugen N, Hegermann J, Giavalisco P, Eubel H, Witte CP, Herde M. Rapid affinity purification of tagged plant mitochondria (Mito-AP) for metabolome and proteome analyses. Plant Physiol. 2020:182(3):1194–1210. https://doi.org/10.1104/pp.19.00736
- Peer WA, Hosein FN, Bandyopadhyaym A, Makamm SN, Otegui MS, Lee GJ, Blakeslee JJ, Cheng Y, Titapiwatanakun B, Yakubov B, et al. Mutation of the membrane-associated M1 protease APM1 results in distinct embryonic and seedling developmental defects in

- *Arabidopsis.* Plant Cell 2009:**21**(6):1693–1721. https://doi.org/10.1105/tpc.108.059634
- Petsalaki EI, Bagos PG, Litou ZI, Hamodrakas SJ. PredSL: a tool for the N-terminal sequence-based prediction of protein subcellular localization. Genomics Proteomics Bioinformatics 2006:4(1):48–55. https://doi.org/10.1016/S1672-0229(06)60016-8
- Sattler SE, Cahoon EB, Coughlan SJ, DellaPenna D. Characterization of tocopherol cyclases from higher plants and cyanobacteria. Evolutionary implications for tocopherol synthesis and function. Plant Physiol. 2003:132(4):2184–2195. https://doi.org/10.1104/pp. 103.024257
- Senkler J, Senkler M, Eubel H, Hildebrandt T, Lengwenus C, Schertl P, Schwarzländer M, Wagner S, Wittig I, Braun HP. The mitochondrial complexome of *Arabidopsis thaliana*. Plant J. 2017:**89**(6): 1079–1092. https://doi.org/10.1111/tpj.13448
- Small I, Peeters N, Legeai F, Lurin C. Predotar: a tool for rapidly screening proteomes for N-terminal targeting sequences. Proteomics 2004;4(6):1581–1590. https://doi.org/10.1002/pmic.200300776
- Søballe B, Poole RK. Microbial ubiquinones: multiple roles in respiration, gene regulation and oxidative stress management. Microbiology (Reading) 1999:145(8):1817–1830. https://doi.org/10.1099/13500872-145-8-1817
- Szymańska R, Kruk J. Plastoquinol is the main prenyllipid synthesized during acclimation to high light conditions in *Arabidopsis* and is converted to plastochromanol by tocopherol cyclase. Plant Cell Physiol. 2010:51(4):537–545. https://doi.org/10.1093/pcp/pcq017
- Tardif M, Atteia A, Specht M, Cogne G, Rolland N, Brugière S, Hippler M, Ferro M, Bruley C, Peltier G, et al. PredAlgo: a new subcellular localization prediction tool dedicated to green algae. Mol Biol Evol. 2012:29(12):3625–3639. https://doi.org/10.1093/molbev/mss178
- **Unden G**. Differential roles for menaquinone and demethylmenaquinone in anaerobic electron transport of *E. coli* and their *fnr*-independent expression. Arch Microbiol. 1988:**150**(5):499–503. https://doi.org/10.1007/BF00422294
- Widhalm JR, Ducluzeau AL, Buller NE, Elowsky CG, Olsen LJ, Basset GJ. Phylloquinone (vitamin K₁) biosynthesis in plants: two peroxisomal thioesterases of Lactobacillales origin hydrolyze 1,4-dihydroxy-2-naphthoyl-CoA. Plant J. 2012;**71**(2):205–215. https://doi.org/10.1111/j.1365-313X.2012.04972.x
- Widhalm JR, van Oostende C, Furt F, Basset GJ. A dedicated thioesterase of the hotdog-fold family is required for the biosynthesis of the naphthoquinone ring of vitamin K₁. Proc Natl Acad Sci U S A. 2009:106(14):5599–55603. https://doi.org/10.1073/pnas.0900738106
- Xu L, Law SR, Murcha MW, Whelan J, Carrie C. The dual targeting ability of type II NAD(P)H dehydrogenases arose early in land plant evolution. BMC Plant Biol. 2013:13(1):100. https://doi.org/10.1186/1471-2229-13-100